



Supplement of

A dynamically based method for estimating the Atlantic meridional overturning circulation at 26° N from satellite altimetry

Alejandra Sanchez-Franks et al.

Correspondence to: Alejandra Sanchez-Franks (alsf@noc.ac.uk)

The copyright of individual parts of the supplement might differ from the article licence.

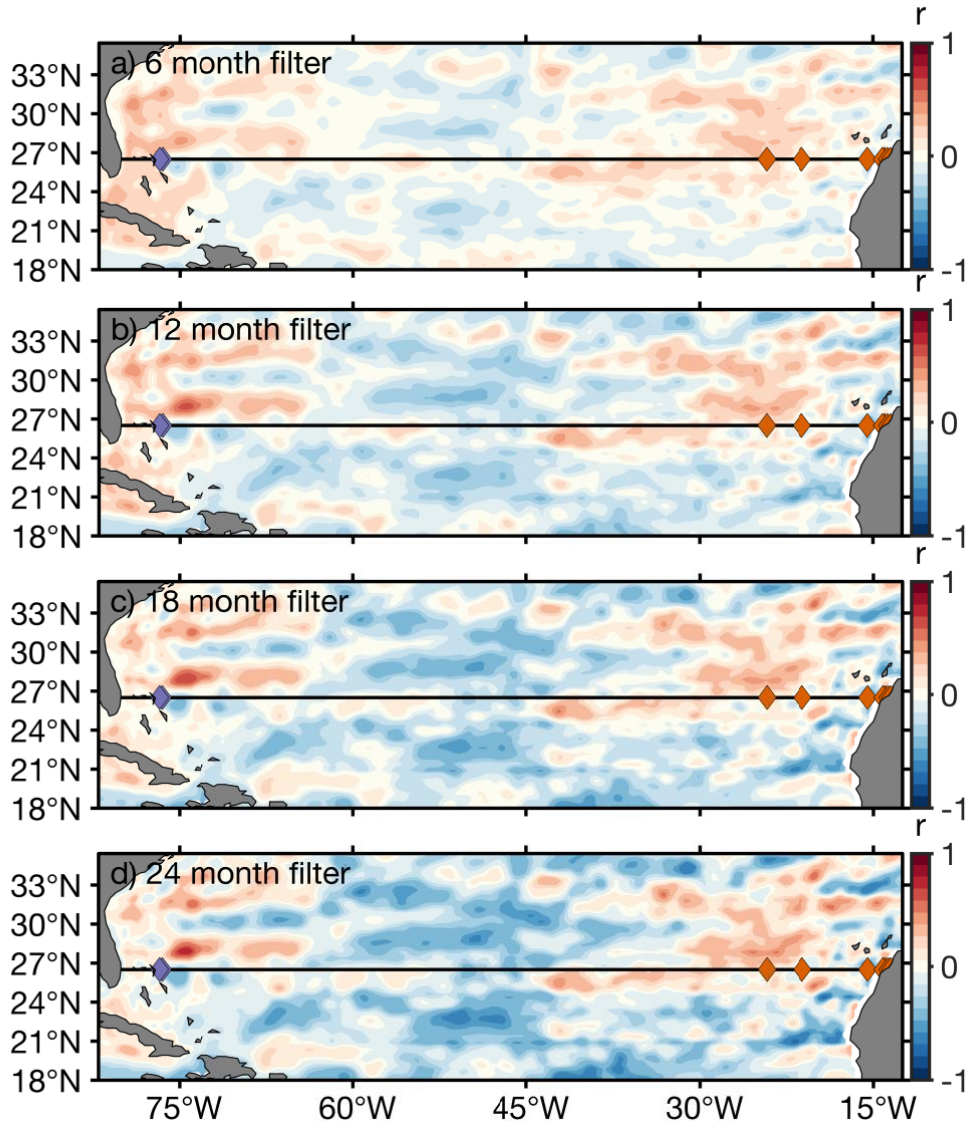


Figure S1. Correlation map between east-west difference in SLA ($\Delta\eta$) and the RAPID upper mid-ocean transport (T_{UMO}), where data has a 6 month Gaussian filter (a), a 12 month Gaussian filter (b), an 18 month Gaussian filter (c), and a 24 month Gaussian filter. Western (purple diamonds) and eastern (orange diamonds) moorings are indicated along the RAPID array (black line).

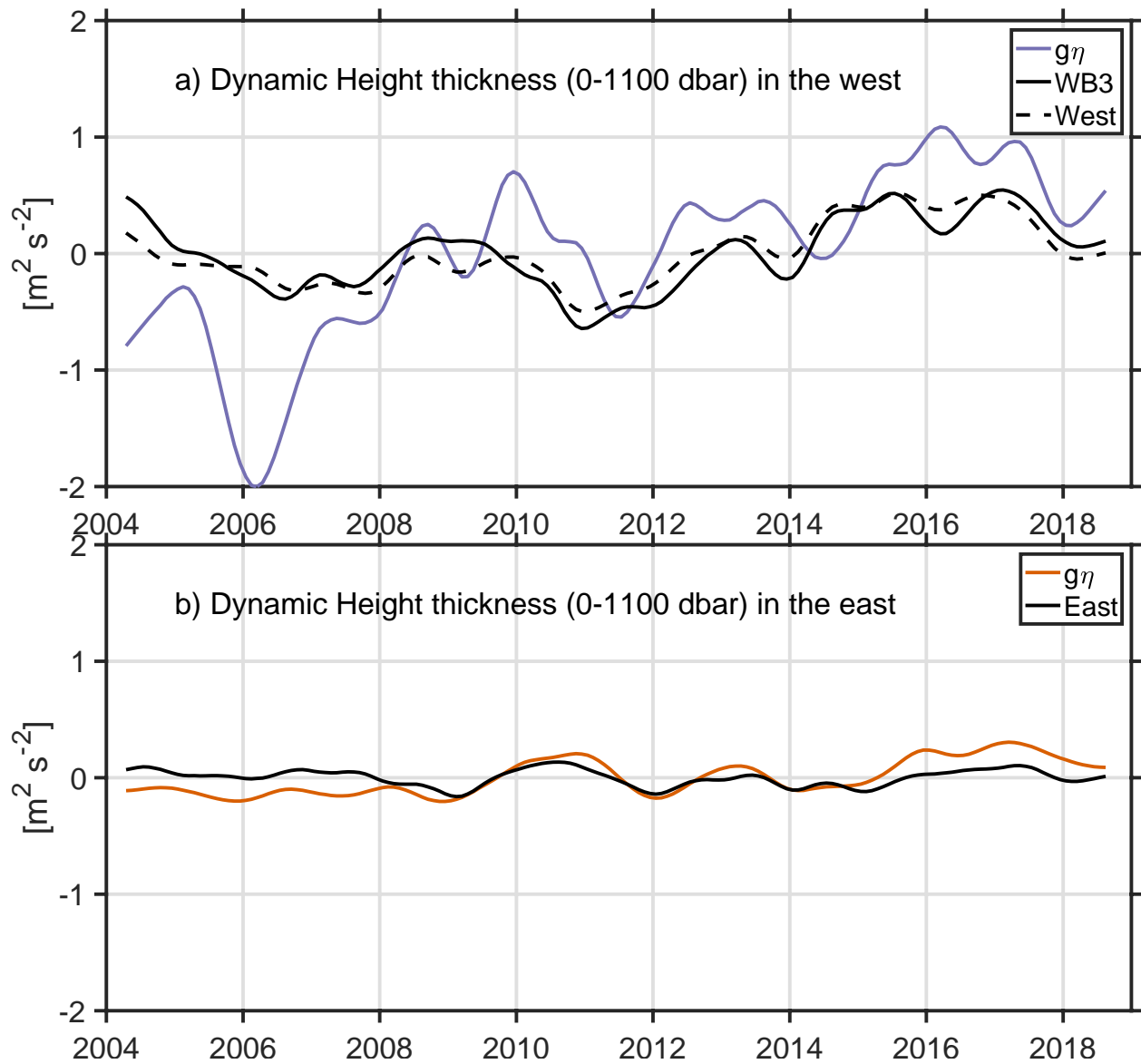


Figure S2. The dynamic height thickness anomaly at moorings (a) WB3 and West, and (b) EB moorings. The dynamic height thickness is compared with the SLA multiplied by gravitational acceleration in the western and eastern basin, respectively. Units in $\text{m}^2 \text{s}^{-2}$.

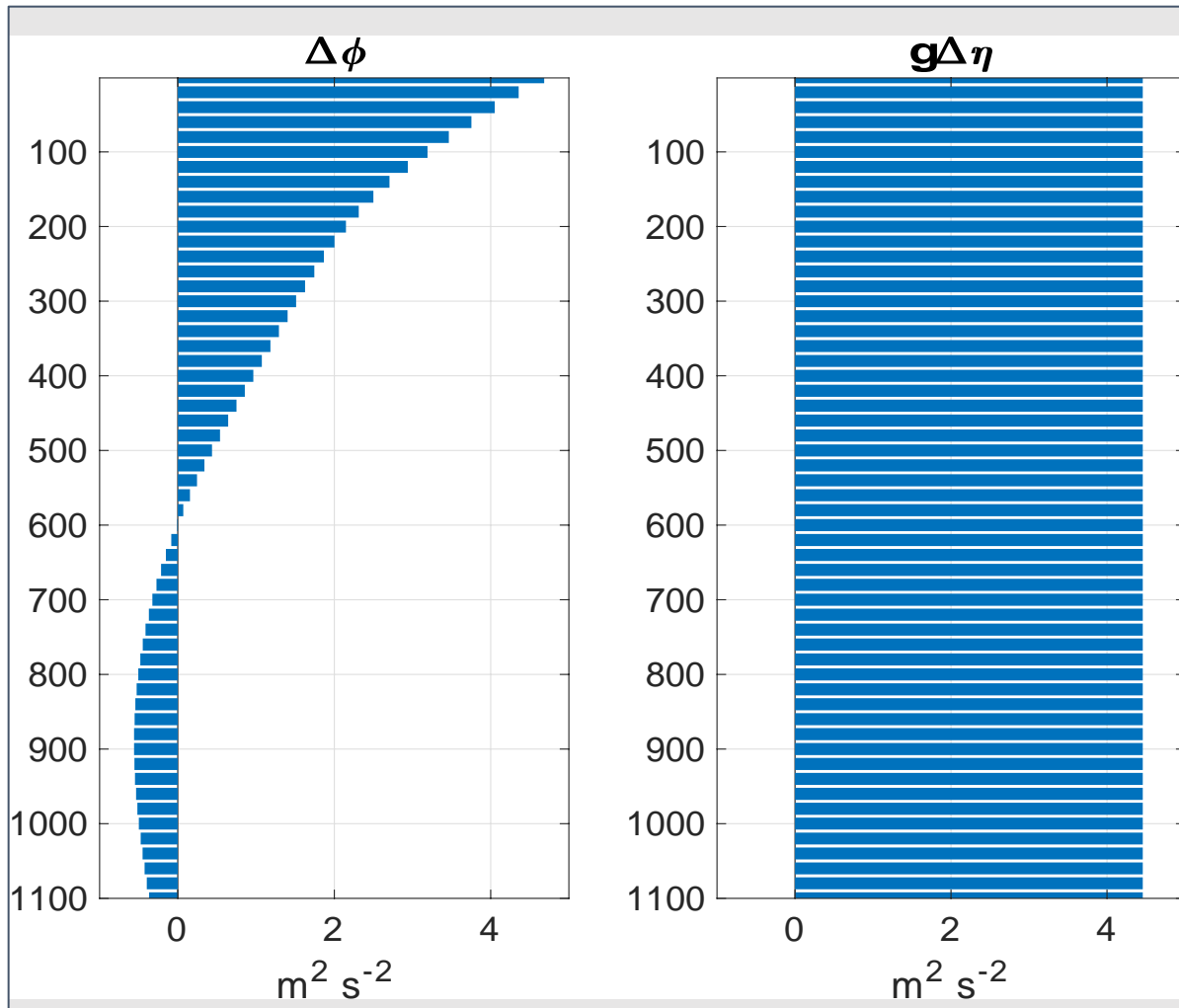


Figure S3. Time averaged east-west difference in dynamic height, $\Delta\phi$ (a), and SLA multiplied by gravitational acceleration, $g\Delta\eta$ (b), at every pressure level. Units in $\text{m}^2 \text{s}^{-2}$.

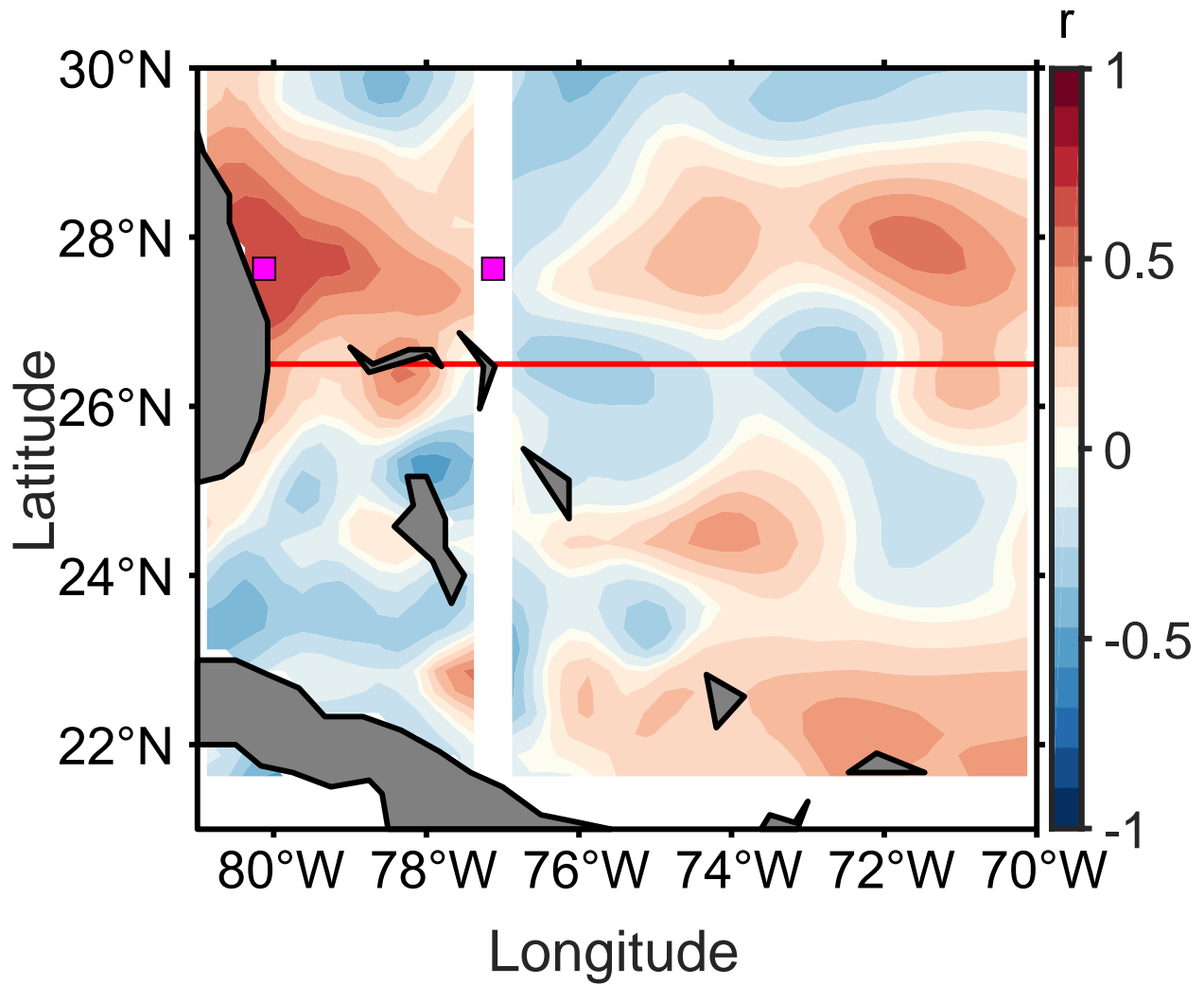


Figure S4. a) Correlation map between east-west difference in SLA ($\Delta\eta$) and the telephone cable Gulf Stream transport (T_{GS}). Magenta squares in the western and eastern part of basin indicate region of maximum correlation between $\Delta\eta$ and T_{GS} .

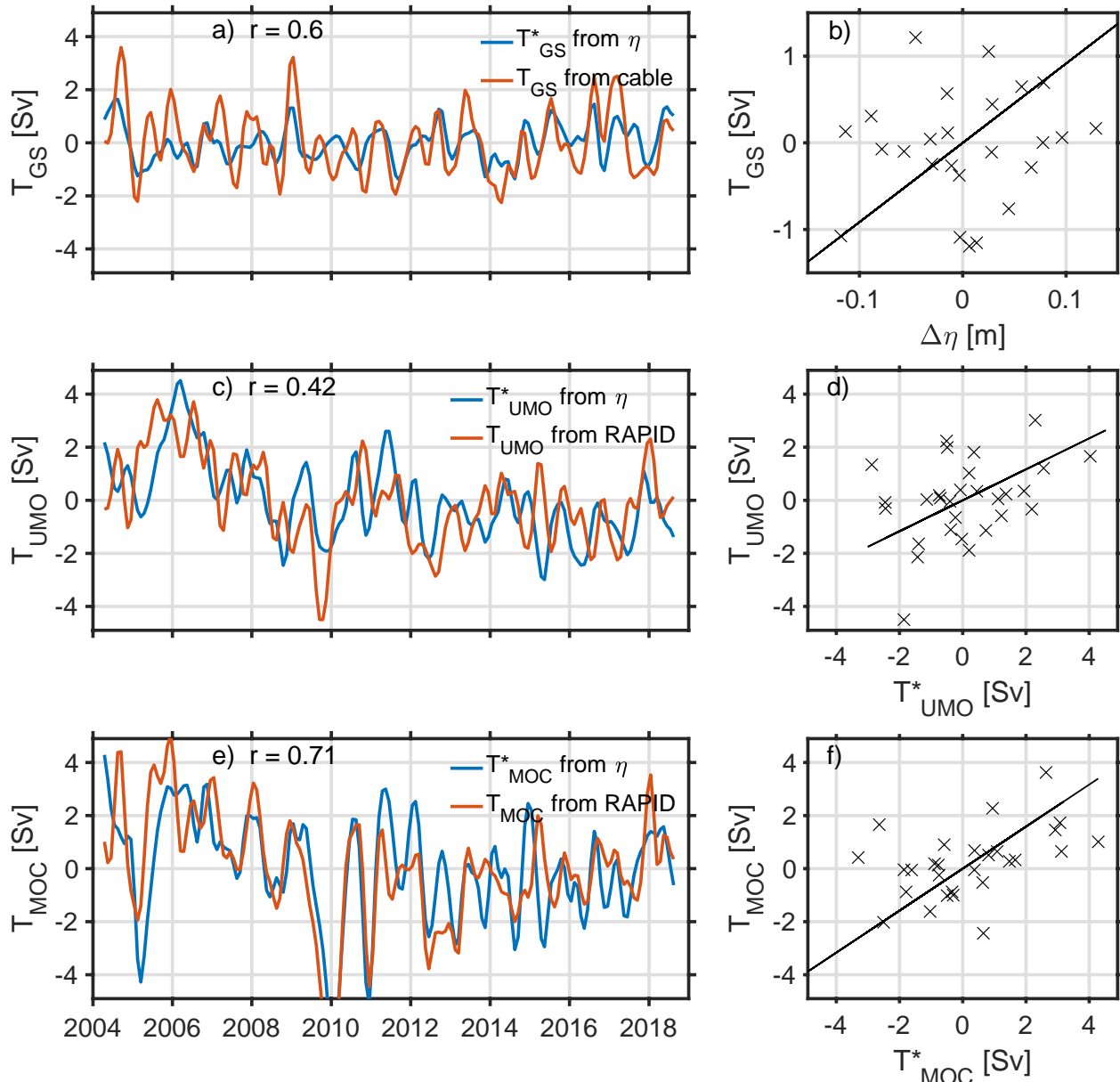


Figure S5. a) Time series of the Gulf Stream transport (T_{GS}) from submarine cables (orange line; Baringer and Larsen, 2001) and the satellite-derived T_{GS}^* estimates as per Eq. (18) (blue line). b) Scatterplot between the east (27.625°N and 77.125°W) - west (27.625°N and 80.125°W) SLA (η) and T_{GS} with the line of best fit linear regression – note y and x axis limits reduced to improve visibility of datapoints. c) RAPID upper mid-ocean transport (T_{UMO} ; orange line) and the satellite-based T_{UMO}^* transport estimates as per Eq. (19) (blue line). d) Scatterplot between the T_{UMO}^* and T_{UMO} with the line of best fit linear regression. e) RAPID upper mid-ocean transport (T_{MOC} ; orange line) and the satellite-based T_{MOC}^* transport estimates as per Eq. (20) (blue line). f) Scatterplot between the T_{MOC}^* and T_{MOC} with the line of best fit linear regression. In (b,d,f) data are subsampled every 6 months. Seasonal annual climatology is removed and a 6-month Gaussian filter is applied to the data. Units in Sv.

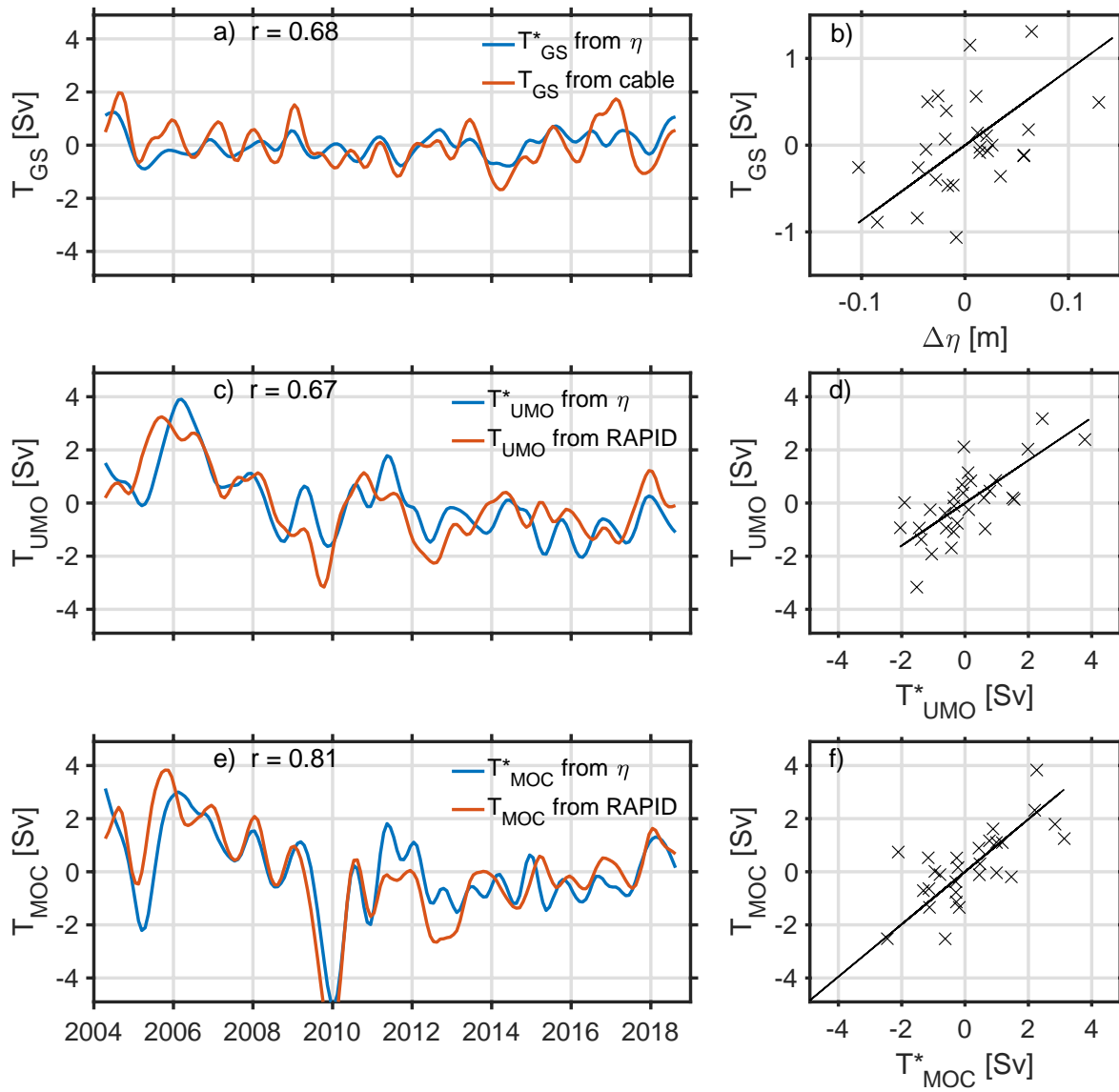


Figure S6. Same as in Figure S6 but using a 12 month Gaussian filter.

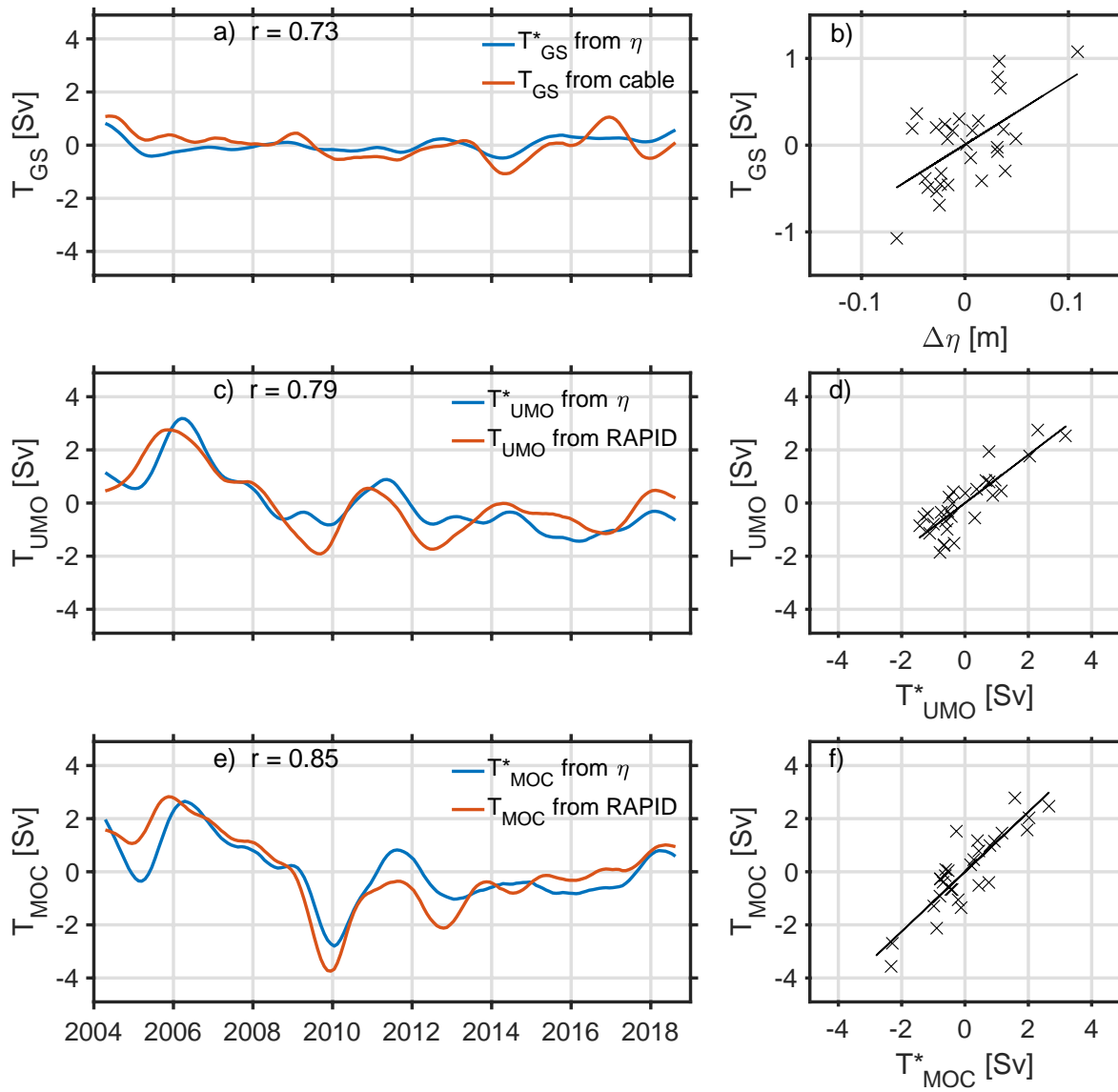


Figure S7. Same as in Figure S6 but using a 24 month Gaussian filter.